Journal of Molecular and Engineering Materials
Vol. 2, No. 2 (2014) 1440009 (7 pages)

DOI: 10.1142/S2251237314400097

World Scientific
www.worldscientific.com

PLASMONIC COLOR FILTERS

GUANGYUAN SI
College of Information Science and Engineering
Northeastern University, Shenyang 110004, China
siguang0323@hotmail.com

YANHUI ZHAO
Department of Engineering Science and Mechanics
The Pennsylvania State University
University Park, PA 16802, USA
yzz127@psu.edu

AH BIAN CHEW* and YAN JUN LIU†
Institute of Materials Research and Engineering
3 Research Link, Singapore 117602, Singapore
**chewab@imre.a-star.edu.sg*
†*liuy@imre.a-star.edu.sg*

Received 19 February 2014
Accepted 4 April 2014
Published 23 May 2014

Plasmon-assisted color filtering devices have drawn increasing attention recently, thanks to their great potential for ultrahigh resolution display technology. In this paper, both transmission and reflection type color filters based on tuning surface plasmon resonance will be summarized. Transmission type color filters using nanohole arrays, nanoslits with grooves, metal–insulator–metal gratings and coaxial apertures will be reviewed first. Then reflective color filters using nanorods with ultrasmall separations will be discussed briefly. We believe more practical achievements of plasmon-based devices will be readily realized in the near future.

Keywords: Color filter; surface plasmon; nanostructures.

1. Introduction

Surface plasmons (SPs), referring to the electromagnetic waves propagating along metallic-dielectric interfaces, have drawn considerable attention over the past 10 years.[1–10] A wide range of practical plasmon-based applications[11–30] have been triggered because of their unique optical properties and particular ability of manipulating light at sub-wavelength scales. Furthermore, since the near-field of electromagnetic waves can be enhanced dramatically using plasmonic nanostructures with different designs, SP-based waveguides are useful for developing devices with ultrahigh sensitivity and figure of merit. Particularly, tuning of SPs in the visible range is critical and essential to develop optical devices like color filters, modulators and sensors. Among all these applications mentioned above, color filters are of special importance because of their great potential for display and imaging. In

digital imaging devices, primary color components are balanced in each pixel to generate desired colors. Using suitable fabrication methods, plasmonic structural color filters working under both transmission and reflection testing modes can be realized. In this paper, color filters using different plasmonic designs will be summarized.

2. Transmission Type Color Filters

The concept of plasmon-assisted color filters started from Ebbesen's hole story.[1] Transmitted light through nanoholes in metallic films can be enhanced at certain wavelengths (also known as extraordinary optical transmission). The surface plasmon resonance (SPR) is strongly dependant on geometric parameters (especially the periodicity) of the hole arrays. For a two-dimensional square- and hexagon-lattice array, the resonant wavelength is determined by[31]

$$\lambda_{\max} = \frac{p}{\sqrt{i^2 + j^2}} \sqrt{\frac{\varepsilon_m \varepsilon_d}{\varepsilon_m + \varepsilon_d}} \tag{1}$$

and

$$\lambda_{\max} = \frac{p}{\sqrt{\frac{4}{3}(i^2 + ij + j^2)}} \sqrt{\frac{\varepsilon_m \varepsilon_d}{\varepsilon_m + \varepsilon_d}}, \tag{2}$$

respectively, where p is the period of the array, ε_m and ε_d are the dielectric constants of the metal and the dielectric material, respectively. i and j are the scattering orders of the array. The periodicity determines the transmission peak positions of SPRs for a given material configuration. As shown in Fig. 1(a), when a broadband light illuminates a nanohole array with 900 nm periodicity patterned in a silver film with 200 nm thickness, several different resonant peaks can be observed in the visible and near-infrared (NIR) bands. Based on this mechanism, color filters using nanohole arrays with varying periodicities have been fabricated to demonstrate the effective tuning of plasmon resonance.[31,32] As shown in Fig. 1(b), red, green and blue (RGB) primary colors can be separated from a broadband light source using nanohole arrays. The corresponding spectra are shown in Fig. 1(c).

One decade later, Ebbesen and coworkers[33] used nanoslits with periodic grooves acting as the antennae to collect the optical signals transmitted through the nanoslits, leading to color filtering effect as shown in Fig. 2(a). Importantly, they demonstrate a useful concept of sorting photons by overlapping the nanograting structures. The working mechanism of the proposed photon detector is shown in Fig. 3(a). The basic unit structures are integrated into a lattice and overlapped with each

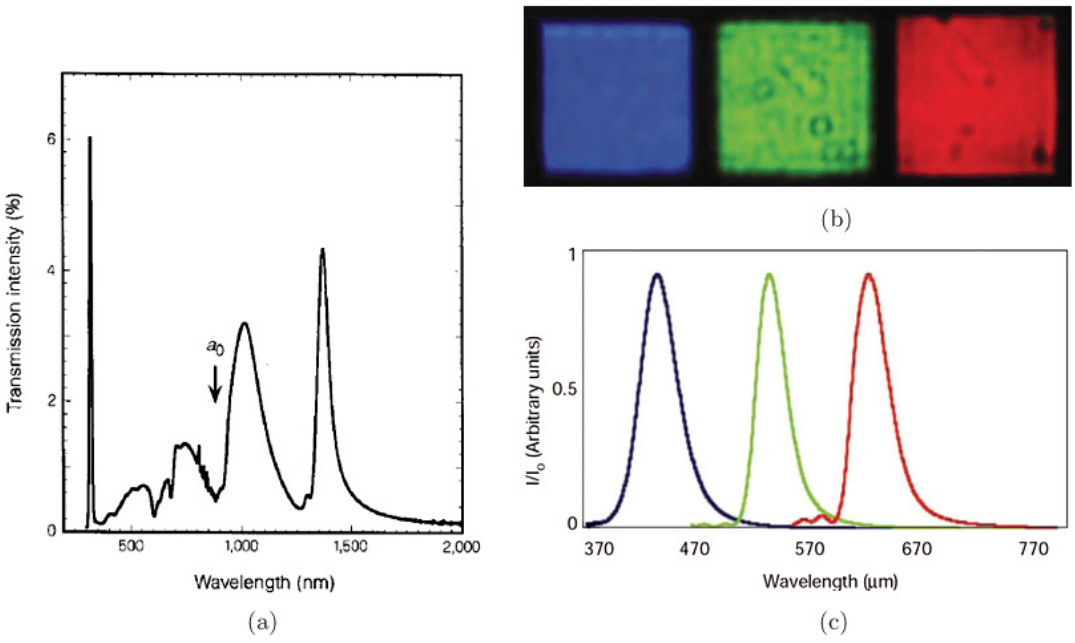

Fig. 1. (a) Transmission of a nanohole array with 900 nm periodicity patterned in a 200 nm thick silver film, (b) RGB colors are filtered out and (c) corresponding spectra for colors shown in (b). Reproduced with permission (Refs. 1 and 32). Copyright 1998 and 2003, NPG (color online).

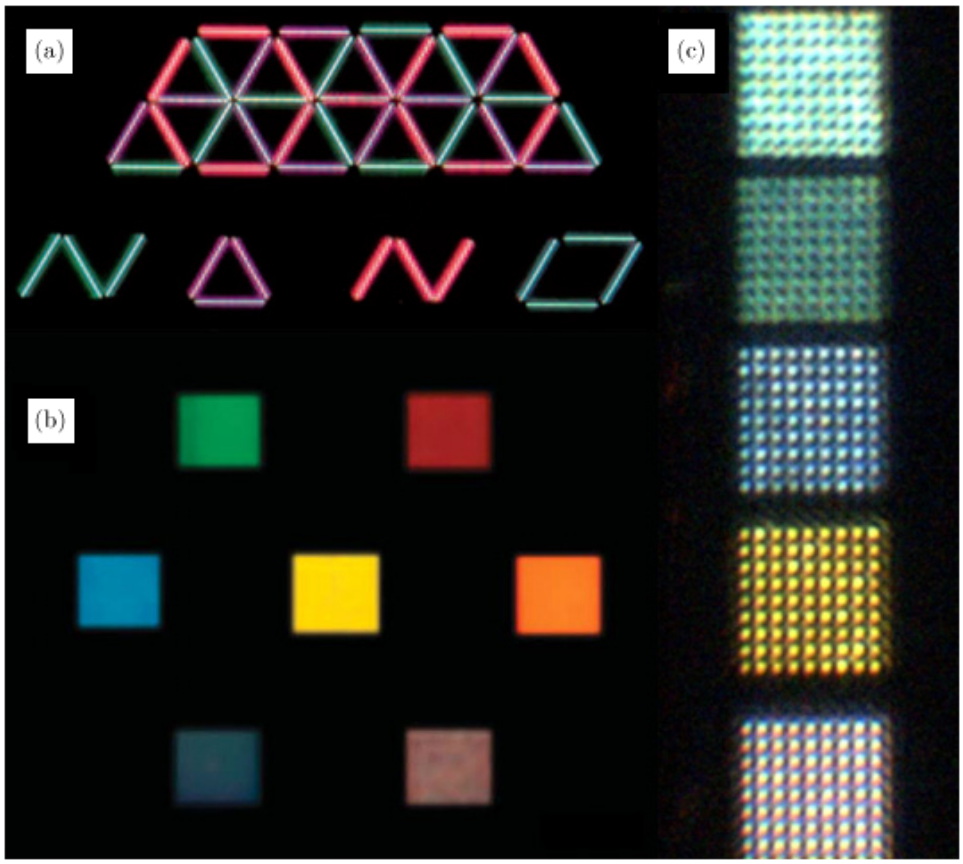

Fig. 2. Color filters under transmission mode using various designs of (a) nanoslits with antenna grooves, (b) MIM strips and (c) coaxial nanorings. (a, b) Reproduced with permission (Refs. 33 and 34). Copyright 2008 and 2010, NPG. (c) Reproduced with permission (Ref. 37). Copyright 2011, AIP (color online).

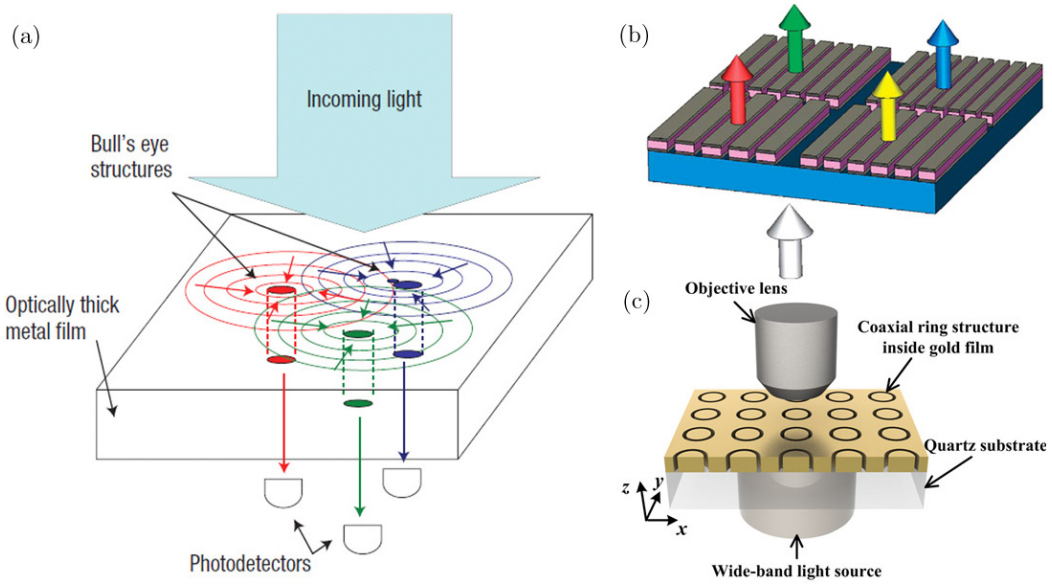

Fig. 3. Working mechanisms and schematics for color filters using (a) nanoslits with antenna grooves, (b) MIM strips and (c) coaxial rings. (a, b) Reproduced with permission (Refs. 33 and 34). Copyright 2008 and 2010, NPG. (c) Reproduced with permission (Ref. 37). Copyright 2011, AIP (color online).

other for spectral filtering and imaging. The transmitted signal is collected by the photodetectors located beneath the metal film. Note that narrow slits with 170 nm width are used here. It is also worth mentioning that the plasmonic structure and photodetector array could be easily integrated into a monolithic image sensing device. Later in 2010, Xu *et al.* used metal–insulator–metal (MIM) strips to filter individual colors out by controlling the pitch of the one-dimensional MIM array,[34] as illustrated in Fig. 2(b). Such structures based on coupled gratings are able to create optical magnetic responses across the whole visible band. The magnetic resonance wavelength is highly dependent on the geometric parameters, enabling different magnetic metamaterial designs at any desired optical frequency bands. Note that, these structures have both magnetic and electric resonances under transverse magnetic (TM) illumination with the magnetic field polarized along the strips. For transverse electric (TE) polarization with the electric field aligned with the strips, the structure exhibits no resonant effects due to the polarization selectivity of such one-dimensional structures.

The schematic view of the proposed structures and working mechanism is illustrated in Fig. 3(b). The device is designed as a sub-wavelength periodic MIM stack array on a magnesium fluoride film with varying periods. For each stack, a 100 nm-thick zinc selenide layer is sandwiched by two 40 nm-thick aluminum layers. The corresponding period of the stack is 360 nm, 270 nm and 230 nm to generate RGB colors. It is also worth mentioning that the design principle can be simply applied to other wavelength ranges, leading to more practical applications.

Most recently, coaxial structures have become an important candidate for single layer metamaterials[35] in the visible range due to their useful potential for ultracompact optical devices. Different from the mechanisms of extraordinary optical transmission observed from sub-wavelength cylindrical nanoholes, such ring-like structures can support propagating modes. Additionally, the cut-off wavelength of a guided mode can be effectively shifted to longer wavelengths when the outer and inner radii are approaching each other. Furthermore, the low group velocity of the fundamental mode gives rise to important applications when materials with large electro-optic coefficients (e.g., lithium niobate) are filled in the cavities between the inner and outer sidewalls of the rings. Importantly, experimental results show that up to 90% transmission through such coaxial apertures can be achieved at visible frequencies.[36] High transmission combined with the fact that the optical response of such structures is almost insensitive to the incident angle makes the coaxial apertures a nearly perfect candidate for high efficiency display and filtering devices.[37]

The color filtering effect of coaxial apertures is shown in Fig. 2(c). Using apertures with fixed period at 1200 nm and different gap width from 40 nm to 200 nm in 40 nm increments, various individual colors are filtered out. The schematic view of the coaxial nanorings is shown in Fig. 3(c). Here, a gold film with fixed thickness (160 nm) fabricated on a quartz substrate is used. A two-dimensional coaxial aperture usually has two transmission peaks, which are cylindrical surface plasmons (CSPs) and planar surface plasmons (PSPs), respectively. CSPs are mostly determined by the structural design and the thickness of the metal film. On the other hand, PSPs are mainly affected by the periods of two-dimensional nanoring gratings. The resonant peaks are a direct result of Fabry–Pérot resonances in a cylindrical cavity formed by a metal film with finite thickness and two end-faces. For a finite metal film with thickness l, the design of the desired transmission peaks can be estimated by the following equation[38]:

$$l = \frac{m\pi - \varphi}{\beta}, \tag{3}$$

where m is the order of the Fabry–Pérot resonance, and β and φ represent the phase of propagation and reflection constant, respectively. When l is constant, the propagation constant β varies with different aperture sizes, and thus further affects the reflection and transmission of the designed aperture.

For both nanoslits and MIM strips, only TM polarized light can be effectively filtered out due to the polarization selectivity of such one-dimensional nanostructures. There are no such limitations for the two-dimensional nanoring color filters. However, relatively low transmission efficiency is the main obstacle for wide technical applications of such devices. Highly efficient color filtering devices are needed.

3. Reflective Color Filters

Using noble metals, electromagnetic waves can be coupled to fabricated nanostructures, resulting in

collective electron oscillations localized in the metallic nanostructure (also known as the localized surface plasmon resonances, LSPRs). The excitation of LSPRs lead to enhanced electromagnetic fields and near-field coupling. Based on the shift of the LSPR wavelength, high performance sensing of refractive index is available in a wide range of applications.[39–41] In particular, the optical response of metallic particles can be tailored for operation at different frequency bands, offering great opportunities for various photonic designs at nanometer scales. The tunability of the LSPR with high performance and sensitivity is therefore important. Additionally, the interaction between electromagnetic waves and metal nanoparticles allows for tight confinement of light and guiding beyond diffraction limit. Coupling between metallic nanorods leads to a significantly enhanced electric field[42] when the neighboring rods are close enough to excite the interaction between different plasmon modes. Resonances depend strongly on the separation between nanorods and the strength of their individual interaction with the incident wave. Therefore, reflection resonances generated at visible frequencies using dense plasmonic periodic nanorod arrays with ultrasmall inter-rod separation to introduce strong near-field coupling and accurate tuning of plasmon resonance across the whole visible band via geometrical control can be realized. For nanorod arrays with ultrasmall separations, strong near-field coupling is enabled between neighboring nanorods involving the sharply evanescent fields tightly confined to the rod tops. By decreasing the inter-rod separation and precisely controlling the periodicity, plasmonic crystal arrays are capable of tuning the plasmon resonance and thus further filtering out individual colors from a broadband light source. In order to generate considerable optical response in the visible range, nanorods with decreasing periodicities from 540 nm to 320 nm in steps of 55 nm are used to filter individual colors out[43] as shown in Fig. 4. As expected, strong optical excitations in the visible band of the spectrum are observed. By changing the periodicity of the nanorod arrays, tuning of the LSPR peak wavelengths between 630 nm (red) to 480 nm (blue) is achieved. One can see that, when the periodicity is 540 nm (40 nm inter-rod separation), a broad resonance is located at around 630 nm. When the periodicity is changed to 485 nm (35 nm inter-rod separation), the resonance peak shifts to 580 nm and reveals a yellow color. When the periodicity is smaller than 430 nm, sharper resonance peaks are obvious and more reflected energy can be observed due to stronger coupling in smaller cavities, presenting as green, cyan and blue, respectively. Additionally, the full width at half maximum undergoes a smooth decrease with gradually reduced periodicity and inter-rod separation from the red color to blue.

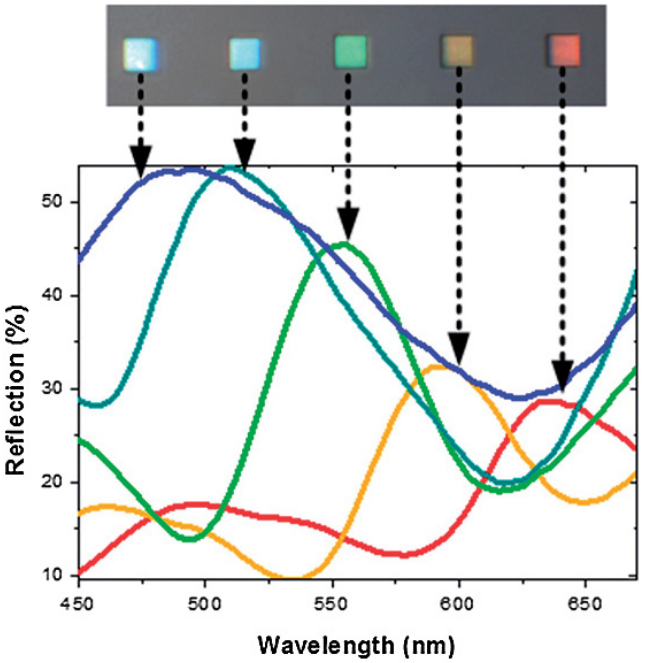

Fig. 4. Color filtering effect and reflection spectra for nanorod arrays with different periods and inter-rod separations. Reproduced with permission (Ref. 43). Copyright 2013, RSC (color online).

4. Summary and Outlook

To conclude, we have reviewed recent progress of structural color filters by tuning the SPR of different plasmonic designs. By using cylindrical nanoholes, nanoslits with antenna grooves, MIM stacks and coaxial nanorings, color filters working under transmission mode are summarized. Complementarily, reflective plasmonic color filters using nanorods with varying periods and separations are demonstrated. Both transmission and reflection structural color filters using various designs take advantage of the unique optical properties of plasmonic nanostructures and pave the way for new generation of display and imaging devices. Importantly, a new category of active plasmonic color filters using liquid crystal[44] or other electro-optical materials (lithium

niobate, for instance) are needed in the near future to achieve switchable optical devices with ultrafast response, which may trigger new opportunities for nanophotonics and optics.

Acknowledgments

This study was partially supported by the NEUQ internal funding (Grant No. XNB201302), Natural Science Foundation of Hebei Province (Grant No. A2013501049), Science and Technology Research Funds for Higher Education of Hebei Province (Grant No. ZD20132011), Fundamental Research Funds for the Central Universities (Grant No. N120323002), Specialized Research Fund for the Doctoral Program of Higher Education (Grant No. 20130042120048), Science and Technology Foundation of Liaoning Province (Grant No. 20131031), and the Scientific Research Foundation for the Returned Overseas Chinese Scholars, State Education Ministry (Grant No. 47-4).

References

1. T. W. Ebbesen, H. J. Lezec, H. F. Ghaemi, T. Thio and P. A. Wolff, *Nature* **391**, 667 (1998).
2. R. de Waele, S. P. Burgos, H. A. Atwater and A. Polman, *Opt. Express* **18**, 12770 (2010).
3. F. I. Baida and D. Van Labeke, *Opt. Commun.* **209**, 17 (2002).
4. F. I. Baida, A. Belkhir, D. Van Labeke and O. Lamrous, *Phys. Rev. B* **74**, 205419 (2006).
5. F. J. Rodríguez-Fortuño, C. García-Meca, R. Ortuño, J. Martí and A. Martínez, *Opt. Lett.* **34**, 3325 (2009).
6. A. Ono, J. Kato and S. Kawata, *Phys. Rev. Lett.* **95**, 267407 (2005).
7. S. Kawata, A. Ono and P. Verma, *Nat. Photon.* **2**, 438 (2008).
8. Y. Liu, G. Bartal and X. Zhang, *Opt. Express* **16**, 15439 (2008).
9. J. A. Fan, C. Wu, K. Bao, J. Bao, R. Bardhan, N. J. Halas, V. N. Manoharan, P. Nordlander, G. Shvets and F. Capasso, *Science* **328**, 1135 (2010).
10. J. B. Lassiter, J. Aizpurua, L. I. Hernandez, D. W. Brandl, I. Romero, S. Lal, J. H. Hafner, P. Nordlander and N. J. Halas, *Nano Lett.* **8**, 1212 (2008).
11. H. Kuwata, H. Tamaru, K. Esumi and K. Miyano, *Appl. Phys. Lett.* **83**, 4625 (2003).
12. J. N. Anker, W. P. Hall, O. Lyandres, N. C. Shah, J. Zhao and R. P. Van Duyne, *Nat. Mater.* **7**, 442 (2008).
13. I. Zorić, E. M. Larsson, B. Kasemo and C. Langhammer, *Adv. Mater.* **22**, 4628 (2010).
14. C. Langhammer, M. Schwind, B. Kasemo and I. Zorić, *Nano Lett.* **8**, 1461 (2006).
15. J. Aizpurua, P. Hanarp, D. S. Sutherland, M. Käll, G. W. Bryant and F. J. García de Abajo, *Phys. Rev. Lett.* **90**, 057401 (2003).
16. P. Nordlander, *ACS Nano* **3**, 488 (2009).
17. S. I. Bozhevolnyi, V. S. Volkov, E. Devaux, J. Y. Laluet and T. W. Ebbesen, *Nature* **440**, 508 (2006).
18. J. C. Weeber, G. Colas-Des-Francs, A. Bouhelier and A. Dereux, *Phys. Rev. B* **83**, 115433 (2011).
19. J. A. Dionne, H. J. Lezec and H. A. Atwater, *Nano Lett.* **6**, 1928 (2006).
20. S. Lal, S. Link and N. J. Halas, *Nat. Photon.* **1**, 641 (2007).
21. Z. Liu, Q. Wei and X. Zhang, *Nano Lett.* **5**, 957 (2005).
22. Z. Liu, Y. Wang, J. Yao, H. Lee, W. Srituravanich and X. Zhang, *Nano Lett.* **9**, 462 (2009).
23. X. Wei, X. Luo, X. Dong and C. Du, *Opt. Express* **15**, 14177 (2007).
24. W. Srituravanich, N. Fang, C. Sun, Q. Luo and X. Zhang, *Nano Lett.* **4**, 1085 (2004).
25. C. Sun, K. Su, J. Valentine, Y. T. Rosa-Bauza, J. A. Ellman, O. Elboudwarej, B. Mukherjee, C. S. Craik, M. A. Shuman, F. F. Chen and X. Zhang, *ACS Nano* **4**, 978 (2010).
26. J. McPhillips, A. Murphy, M. P. Jonsson, W. R. Hendren, R. Atkinson, F. Höök, A. V. Zayats and R. J. Pollard, *ACS Nano* **4**, 2210 (2010).
27. P. Offermans, M. C. Schaafsma, S. R. J. Rodriguez, Y. Zhang, M. Crego-Calama, S. H. Brongersma and J. G. Rivas, *ACS Nano* **5**, 5151 (2011).
28. F. Hao, P. Nordlander, Y. Sonnefraud, P. Van Dorpe and S. A. Maier, *ACS Nano* **3**, 643 (2009).
29. O. Vazquez-Mena, T. Sannomiya, L. G. Villanueva, J. Voros and J. Brugger, *ACS Nano* **5**, 844 (2011).
30. G. Si, Y. Zhao, J. Lv, F. Wang, H. Liu, J. Teng and Y. J. Liu, *Nanoscale* **5**, 4309 (2013).
31. Q. Chen and D. R. S. Cumming, *Opt. Express* **18**, 14056 (2010).
32. W. L. Barnes, A. Dereux and T. W. Ebbesen, *Nature* **424**, 824 (2003).
33. E. Laux, C. Genet, T. Skauli and T. W. Ebbesen, *Nat. Photon.* **2**, 161 (2008).
34. T. Xu, Y. K. Wu, X. G. Luo and L. J. Guo, *Nat. Commun.* **1**, 1058 (2010).
35. S. P. Burgos, R. de Waele, A. Polman and H. A. Atwater, *Nat. Mater.* **9**, 407 (2010).
36. Y. Poujet, J. Salvi and F. I. Baida, *Opt. Lett.* **32**, 2942 (2007).
37. G. Si, Y. Zhao, H. Liu, S. Teo, M. Zhang, T. J. Huang, A. J. Danner and J. Teng, *Appl. Phys. Lett.* **99**, 033105 (2011).

38. B. Heshmat, D. Li, T. E. Darcie and R. Gordon, *Opt. Express* **19**, 5912 (2011).
39. K. Lodewijks, W. Van Roy, G. Borghs, L. Lagae and P. Van Dorpe, *Nano Lett.* **12**, 1655 (2012).
40. M. Svedendahl, S. Chen, A. Dmitriev and M. Kall, *Nano Lett.* **9**, 4428 (2009).
41. M. H. Lee, H. Gao and T. W. Odom, *Nano Lett.* **9**, 2584 (2009).
42. G. A. Wurtz, W. Dickson, D. O'Conner, R. Atkinson, W. Hendren, P. Evans, R. Pollard and A. V. Zayats, *Opt. Express* **16**, 7460 (2008).
43. G. Si, Y. Zhao, J. Lv, M. Lu, F. Wang, H. Liu, N. Xiang, T. J. Huang, A. J. Danner, J. Teng and Y. J. Liu, *Nanoscale* **5**, 6243 (2013).
44. G. Si, Y. Zhao, E. S. P. Leong and Y. J. Liu, *Materials* **7**, 1296 (2014).